

# Seasonal variability and trends of volatile organic compounds in the lower polar troposphere

M. Gautrois, T. Brauers, R. Koppmann, F. Rohrer, and O. Stein

Institut für Chemie und Dynamik der Geosphäre, Institut II: Troposphäre, Forschungszentrum Jülich, Jülich, Germany

J. Rudolph

Chemistry Department and Centre for Atmospheric Chemistry, York University, Toronto, Ontario, Canada

[1] Measurements of the atmospheric mixing ratios of 10 nonmethane hydrocarbons (NMHC) and four halocarbons (methyl chloride, dichloromethane, trichloroethene, and tetrachloroethene) were conducted between January 1989 and July 1996 at Alert (Canadian Arctic, 82°27'N, 62°31'W). About 270 canister samples were analyzed covering the 7-year period with an average frequency of about one sample every 9 days. The mixing ratios of these volatile organic compounds (VOC) exhibit considerable variability, which can partly be described by systematic seasonal dependencies. The highest mixing ratios were always observed during winter. During spring, the mixing ratios decrease for some compounds to values near the detection limit. The amplitudes of the seasonal variability, the time of the occurrence of the maxima, and the relative steepness of the temporal gradients show a systematic dependence on OH reactivity. The steepest relative decrease is less than 1% d<sup>-1</sup> for methyl chloride, increasing to about 4% d<sup>-1</sup> for highly reactive VOC. Similarly, the highest relative increase rates vary between 0.5% d<sup>-1</sup> for VOC with low reactivity to 4% d<sup>-1</sup> for reactive VOC. With the exception of ethyne, toluene, and methyl chloride the concentrations of all measured VOC decrease during the studied period, although this decrease is not always statistically significant. In general, the largest changes were found for the most reactive VOC, although the seemingly random overall variability observed for these compounds results in substantial uncertainties. For the less reactive VOC (ethane, benzene, and propane) the average relative annual decrease rate is in the range of a few percent per year. Dichloromethane and tetrachloroethene showed a decrease of 4 and 14% yr<sup>-1</sup>, respectively. The average decrease rate for the other alkanes is in the range of some 10% yr<sup>-1</sup>, indicating a substantial change of emission rates during this period. A likely explanation is a reduction in VOC emissions in the area of the former Soviet Union, most likely Siberia, as a consequence of the recent major economic changes in this region. The measurements were compared with the results of chemical transport models' simulations using the Emission Database for Global Atmospheric Research NMHC emission inventory. Although the model captures most of the main features of the shapes of the seasonal cycles of the NMHC, the results clearly show that model estimates are consistently too low compared to the observations. Most likely this is the consequence of an underestimate of the NMHC emission rates in the emission inventory. INDEX

TERMS: 0322 Atmospheric Composition and Structure: Constituent sources and sinks; 0365 Atmospheric Composition and Structure: Troposphere—composition and chemistry; 0368 Atmospheric Composition and Structure: Troposphere—constituent transport and chemistry; KEYWORDS: volatile organic compounds, halogenated compounds, Arctic troposphere, trends, seasonal variability

**Citation:** Gautrois, M., T. Brauers, R. Koppmann, F. Rohrer, O. Stein, and J. Rudolph, Seasonal variability and trends of volatile organic compounds in the lower polar troposphere, *J. Geophys. Res.*, 108(D13), 4393, doi:10.1029/2002JD002765, 2003.

## 1. Introduction

[2] Measurements of organic trace gases, particularly nonmethane hydrocarbons (NMHC), have become increasingly valuable to understand important tropospheric pro-

cesses, both for transport and chemistry. Especially, long-term measurement series at remote locations have been instrumental in improving our knowledge on tropospheric sources and sinks of organic trace gases [Ehhalt et al., 1991; Rudolph et al., 1992; Montzka et al., 1996; Derwent et al., 1998; Khalil and Rasmussen, 1999]. However, the number of measurement series that allow determination of repre-

sentative seasonal cycles or trends is still very limited. Trace gases with short atmospheric residence times (less than a few months) show high temporal and spatial variability. In combination with the limited available data sets this results in substantial uncertainties of quantitative information derived from ambient observations.

[3] One of the problems that plague the interpretation of volatile organic compounds (VOC) measurements at remote locations is differentiating between large-scale and local effects. Especially for compounds with short atmospheric residence times and no secondary formation processes, even very small local emission rates can have a substantial impact on the observations. The temporal, and consequently also the spatial scale, that is relevant for the interpretation of VOC concentrations obviously depend on the atmospheric lifetimes and thus the reactivity of the studied compound. The rate constants for the reaction of VOC with OH-radicals, the most important removal process for nearly all VOC, cover several orders of magnitude [cf. Atkinson *et al.*, 1997a, 1997b], the corresponding lifetimes range from several months or longer to less than an hour. As a consequence, observations of VOC at a given location will, depending on the individual VOC, represent spatial scales ranging from some hundred to several thousand kilometers. This complicates the interpretation of seasonal variations and secular trends, but also presents an opportunity to derive insight into the different temporal and spatial regimes that determine the trace gas levels at the measurement location.

[4] In this paper we present results of NMHC mixing ratios determined during a period of 7 years at Alert, a remote location in the Canadian Arctic. We also include measurements of some halocarbons since their atmospheric lifetimes often are somewhat longer, but still in the same range as those of most NMHC.

## 2. Experiment

### 2.1. Sampling Site

[5] The samples were collected at the Baseline Observatory of the Global Atmospheric Watch Station at Alert, Canada ( $82^{\circ}27'N$ ,  $62^{\circ}31'W$ ) between 1989 and 1996. Samples were only collected outside the so-called arctic tropospheric ozone depletion episodes, which are characterized by a strong reduction of ozone concentrations in the lowest troposphere. The station is located 6 km south of the Canadian Forces Station at Alert at the northern rim of the Hazen Plateau at an altitude of about 200 m above sea level. Figure 1 shows the location of Alert in the Canadian Arctic and a detailed map of the surroundings of the sampling site. The area is covered with snow for almost 10 months of the year. During summer time the land is sparsely covered with polar desert vegetation. Alert experiences 106 days of full darkness (30 October to 13 February), 153 days of 24-hour daylight (7 April to 7 September) and two 53-day transition periods. The mean annual temperature is  $-18^{\circ}C$  and only in July and August the monthly mean temperatures are above the freezing point. Details of the climatology for Alert can be found in the *Canadian Baseline Program* [1999].

### 2.2. Sampling Procedure

[6] Whole air grab samples were collected in evacuated 2 l electropolished one-valve stainless steel canisters. All

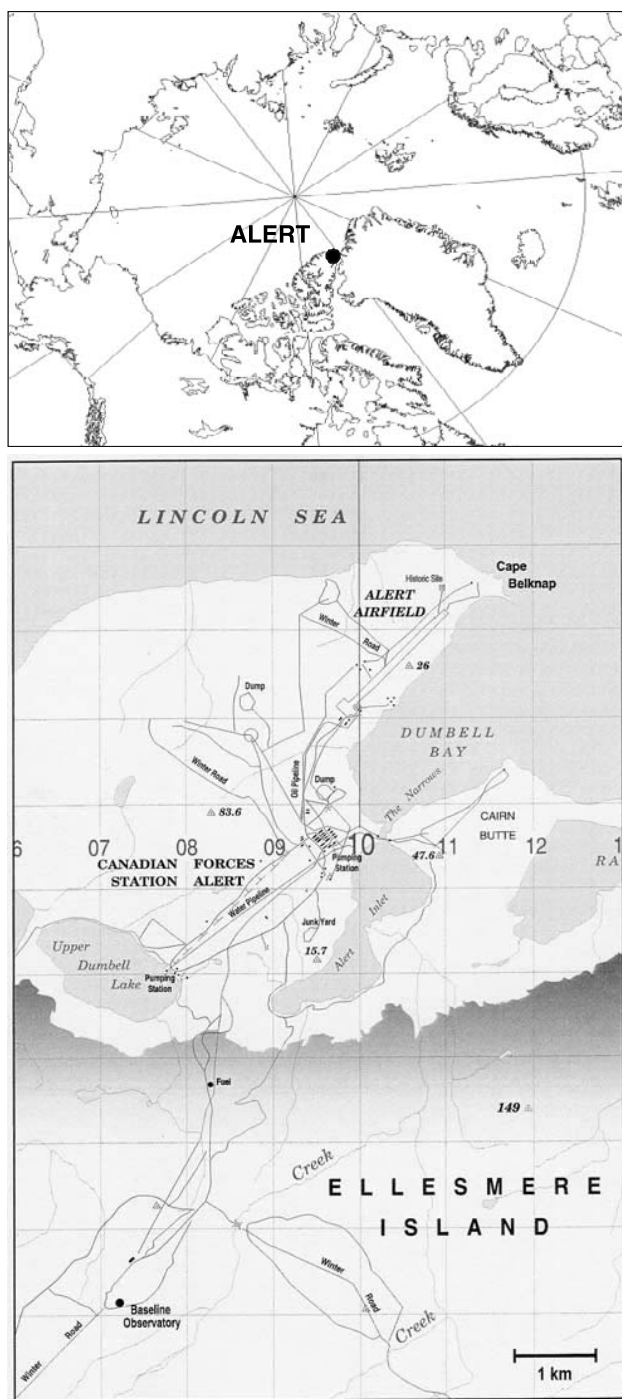


**Figure 1.** Location of Alert in the Canadian Arctic ( $82^{\circ}N$ ,  $62^{\circ}W$ ). The samples were collected at the Baseline Observatory of the Global Atmospheric Watch (GAW) station. The station is located 6 km south of Alert at the Hazen Plateau (see solid circle in upper map).

canisters were carefully conditioned and leak tested before being sent to Alert. Only canisters with a leak rate of less than  $5 \times 10^{-8}$  hPa l s $^{-1}$  were used for sampling. This leak rate results in a maximum total leakage of less than 0.5% of the sample volume for the typical storage and transportation

time of 6 months. This leak rate is valid for a pressure difference of 1 atm (1013 hPa). Since after sampling the pressure difference will be very small our estimate is a conservative upper limit. Even if the hydrocarbon mixing ratios of the contaminant air are 2 orders of magnitude higher than those in the sampled air, this leak rate would result in a contamination that is less than 0.5% of the sample mixing ratios.

[7] The conditioning procedure consisted of four steps. (1) Evacuation with a turbomolecular pump to a final pressure of  $<1 \times 10^{-6}$  hPa for 15 hours at 403 K, (2) filling the evacuated canister with nitrogen of high purity (>99.999%), humidified at 298 K with high-purity water (Milli-Q Water), (3) baking the filled canister for at least 6 hours at 353 K, and (4) evacuation with a turbomolecular pump to a final pressure of about  $1 \times 10^{-6}$  hPa for more than 6 hours at ambient temperature.

### 2.3. Sample Analysis

[8] The samples were analyzed for NMHC and halocarbons with two different gas chromatographic systems both equipped with a flame ionization detector and an electron capture detector. The samples were preconcentrated at liquid nitrogen temperature on a stainless steel sample loop (150 mm length, ID 2 mm) packed with glass beads (60/80 mesh). The samples taken between January 1989 and January 1995 were analyzed using a dual oven gas chromatograph (Sichromat II, Siemens, Germany) with a combination of different columns to separate the VOC in the sample into a light ( $C_2$ - $C_4$ ) fraction, which also included water and carbon dioxide, and a higher molecular weight ( $C_5$  and heavier) fraction. This separation into two fractions was done on a 10-m DB-PS column (J&W,  $L = 10$  m, ID = 0.32 mm), which at 283 K retained the heavy fraction. Water, carbon dioxide, and the light VOC fraction were transferred to and subsequently separated on a packed column ( $L = 6$  m, ID = 0.8 mm, Porapak QS 100/120 mesh). The temperature of this column was initially held at 283 K for 20 min and then increased to 448 K at a rate of  $5 \text{ K min}^{-1}$ . Carrier gas is nitrogen with a flow rate of  $19 \text{ cm}^3 \text{ min}^{-1}$ . The heavy fraction was transferred to a capillary column (RTX-1,  $L = 105$  m, ID = 0.32 mm). To reduce peak broadening this capillary column was cooled during transfer to a temperature of 173 K. After completion of the transfer, the capillary column was rapidly heated to 303 K, held at this temperature for 20 min and then the temperature was increased to 423 K at a rate of  $1.5 \text{ K min}^{-1}$ . Finally, the capillary column temperature was rapidly ( $20 \text{ K min}^{-1}$ ) increased to 503 K. Carrier gas for the capillary column is helium with a flow rate of  $1.3 \text{ cm}^3 \text{ min}^{-1}$ . The time for a complete GC run is 3 h 30 min. This measurement technique is similar to the one described by Ramacher *et al.* [1997]. Samples from the last two measurement series (March 1995–July 1996) were analyzed on a GasPro GSC column ( $L = 60$  m, ID = 0.32 mm) at a helium carrier gas flow rate of  $3.8 \text{ cm}^3 \text{ min}^{-1}$ . The initial temperature of 275 K was held for 6.5 min, then the column temperature was increased to 503 K with a rate of  $5 \text{ K min}^{-1}$ , and finally raised to 533 K with  $10 \text{ K min}^{-1}$ . The time required for this type of analysis was 1 h 45 min. Further details of this system are described by Ramacher *et al.* and Gautrois and Koppmann [1999].

[9] The atmospheric mixing ratios were determined relative to a reference air with known VOC mixing ratios. The VOC mixing ratios in the reference air ranged from several parts per trillion (ppt) to a few parts per billion (ppb), comparable to typical nonurban levels. The VOC mixing ratios in the reference air were calibrated by comparison with ppb or ppt level mixtures prepared by a three-step static dilution of pure VOC with synthetic air.

[10] In order to determine the electron capture detector response function for the individual halogenated hydrocarbons, different volumes of a well-characterized air mixture were analyzed. For methyl chloride, a reference air of known composition was used. For the other halogenated compounds (dichloromethane, trichloroethene, and tetrachloroethene) mixtures with defined composition were prepared using a diffusion chamber [Gautrois and Koppmann, 1999]. The injected amounts of analyte were comparable to the typical range used for analysis of atmospheric air samples.

[11] Blank values were determined by following the analytical procedure used for measurements but without injection of a sample. For the studied compounds no blank peaks could be detected. Thus the theoretical detection limits can be calculated from the baseline noise. The  $3\sigma$  theoretical detection limits as well as the reproducibility determined from repeat analysis of ambient background samples are given in Table 1 for the NMHC and in Table 2 for the halocarbons.

### 2.4. Rejection of Potentially Contaminated Samples

[12] For each of the samples, the mixing ratios were checked for indications of contamination by local anthropogenic sources such as evaporation of fuel, exhaust from power generators, snowmobiles, and air traffic. Indeed, some canisters showed signs of contamination with elevated mixing ratios of carbon monoxide, ethyne, and higher molecular weight NMHC. Also, occasionally high levels of halogenated hydrocarbons such as dichloromethane, trichloroethene, and tetrachloroethene were observed. In very few of the samples, the mixing ratios of some compounds were up to a factor of 30 higher than the average from all samples. Contamination by local anthropogenic emissions with a similar pattern has also been observed by Ramacher *et al.* [1999] during field measurements on Spitsbergen.

[13] To minimize the impact of local contamination effects, we eliminated all samples showing unusually high mixing ratios for any of the compounds mentioned above. A mixing ratio was considered to be unusually high if it exceeded the average of the previous and the following sample by more than a factor of 2. Based on this criterion, in total 15 of the 284 samples, corresponding to about 5% of all samples, were excluded. Thus 269 whole air samples remained covering the 7-year study period. This corresponds to an average of nearly 40 samples each year.

## 3. Results and Discussion

### 3.1. Time Series

[14] Figure 2 shows time series of the hydrocarbon and halocarbon mixing ratios. The red line is a fit to the data obtained by the parameterization given below. In all the time series a clear periodic seasonal cycle can be seen.

**Table 1.** Detection Limits ( $3\sigma$ ) and Reproducibility of Nonmethane Hydrocarbons Measurements

Compound	Mean and Standard Deviation of Mixing Ratios of the Reference Air Sample Based on Three to Five Calibrations Over a Period of 3.5 Years, ppt		Reproducibility Derived From 58 Repeat Measurements of the Reference Air Sample, %	Reproducibility Based on Repeat Analysis of Samples, %	Detection Limit Based on Mean Sample Volume (1110 cm <sup>3</sup> ), ppt
Ethane	2885	±5%	3	2	4
Ethyne	1045	±6%	4	17	5
Propane	1485	±3%	3	4	7
<i>i</i> -Butane	575	±6%	3	18	4
<i>n</i> -Butane	1081	±3%	4	10	4
<i>i</i> -Pentane	940	±5%	3	26	5
<i>n</i> -Pentane	585	±5%	5	18	3
<i>n</i> -Hexane	257	±15%	27	29	4
<i>n</i> -Heptane	84	±8%	22	18	2
Benzene	423	±8%	8	12	2
Toluene	1127	±7%	10	26	5

Furthermore, there is some indication for a secular trend. However, due to the random variability, which is superimposed on the systematic components of the time series, a clear identification of the details of the seasonal periodicity and the secular trend is not trivial.

[15] We therefore fitted our data to a function that allows a quantitative description of the periodic behavior and a systematic linear trend. In order to minimize the covariance between the fit parameters,  $Y(t)$  was normalized to an average of one by division through the average of  $Y(t)$ ,  $\langle Y(t) \rangle$ .

[16] The shape of the seasonal cycles is described by the following function:

$$Y_N(t) = Y(t)/\langle Y(t) \rangle = 1 + \beta Z^{-1} \cdot (C_1 + C_2 \cos(\omega t + \phi)). \quad (1)$$

We used a fixed  $\omega = 2\pi/365.25 \text{ d}^{-1}$ , corresponding to a 1-year periodicity. The inverse Fisher–Z transformation ( $\tanh$ )  $Z^{-1}(X)$  maps  $[-\infty, +\infty]$  into  $[-1, +1]$ :  $Z^{-1}(X) = (e^{2X} - 1)/(e^{2X} + 1)$ . The parameters  $\beta$ ,  $\varphi$ ,  $C_1$ , and  $C_2$  are determined by the fit procedure. The time  $t$  is given relative to the reference date of 1 January 1994, approximately the midpoint of the study period.

[17] This function allows to describe different periodic behaviors for a given  $\cos(\omega t + \varphi)$  by varying only three parameters: With  $C_1 = 0$ ,  $C_2 < 1$ , and  $\beta > 1$  a nearly cosine shape is obtained, while using  $C_1 < 1$ ,  $C_2 > 1$ , and  $\beta = 1$  results in a nearly rectangular function. Setting  $C_1 = C_2 < 1$  and  $\beta = 1$  provides periods of high and low values with different length.

[18] Using  $C_0$  as the mixing ratio on the reference date (1 January 1994) and a linear long-term trend given by  $1 + \alpha t$ , we obtained the following function:

$$M(t) = C_0 Y_N(t, C_1, C_2, \phi, \beta)(1 + \alpha t). \quad (2)$$

Equation (2) represents a six-parameter function of  $t$ . We fitted this function to the observations using a nonlinear least squares fit minimizing

$$\chi^2 = \sum (C(t_i) - M(t_i))^2.$$

The fit results (Table 3) show a wide range of different values for the trend and seasonal variation. Figure 3 compares the derived annual variation of the NMHC and the chlorinated compounds with the monthly averages of the observations. All compounds show an increase in October/November and a decrease between March and May. Details of the seasonal variability will be discussed below.

### 3.2. Bootstrap Analysis

[19] Since day-to-day variations cannot be parameterized with equation (1), we applied a Bootstrap analysis to derive an estimator of the errors of the fit parameters, most importantly, the trend parameter  $\alpha$ . Bootstrap (resampling) techniques were first introduced by *Efron* [1982]. It was shown for a number of problems that this allows the calculation of consistent estimators for the statistical errors of fitted parameters [*Efron and Tibshirani*, 1983; *Davidson and Hinkley*, 1997; *Press et al.*, 1992]. The basic idea of a bootstrap procedure is to generate a large number ( $N > 100$ ) of new data sets  $D_1 \dots D_N$  of the same size as the original data set  $D_0$ .

**Table 2.** Detection Limits ( $3\sigma$ ) and Reproducibility of Chlorocarbon Measurements

Compound	Mixing Ratios and Uncertainties of Reference Air Sample, ppt		Reproducibility of Air Mixture (ALU49965) Based on Five Measurements (1782 ml), %	Reproducibility Based on Repeat Analysis of Samples, %	Detection Limit at Mean Volume of Measurement (1110 ml), ppt
Methyl chloride	361	±18%	2	28	4
Dichloromethane	312	±30%	2	7	9
Trichloroethene	38	±4%	3	22	0.2
Tetrachloroethene	53	±6%	3	10	0.02

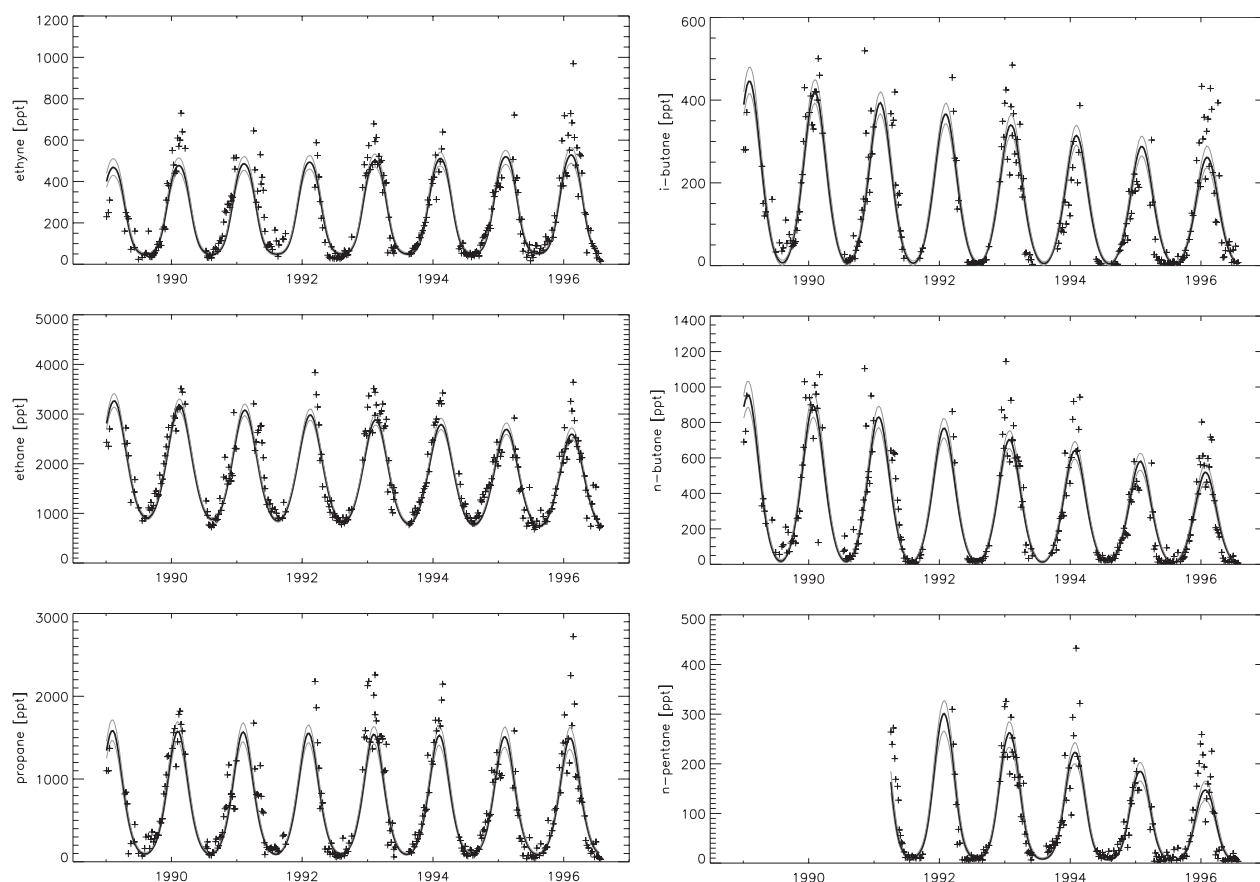


**Figure 2.** Time series of the mixing ratios of selected nonmethane hydrocarbons (NMHC) and chlorocarbons at Alert between 1989 and 1996. (See color version of this figure in the HTML.)

These resampled data sets are created by randomly drawing from the original data set without removing the selected data point from the original data set. Thus every bootstrap data set consists of a random number of points which are missing from the original data set, and a random number of points occurring once, twice, etc., with the overall number of data points being identical to that in the original data set.

[20] Each bootstrap data set is then evaluated by the same fitting procedure as the original data set and the estimator for the fitted parameter vector is saved. Finally, the distribution of different fit parameters is evaluated by calculating the mean and standard deviation, the latter representing the estimated error of the fitted parameter.

[21] For the time series analyzed here, the number of resampled data sets,  $N$ , was set to 200 and we studied the frequency distribution of the trend parameter  $\alpha$ . For all compounds this frequency distribution showed a nearly normal distribution and thus can be characterized by its mean and standard deviation (Table 4). The obtained mean values of the 200 fits to the resampled data sets match the slope value obtained in the fit of the original data, which means that the bootstrap method is a consistent way to estimate the value of the slope.

### 3.3. Comparison With Other Data Sets

[22] Our measurements also included carbon dioxide, carbon monoxide, and methane. However, for these three compounds very detailed measurements series are available

[Blake and Rowland, 1988; Steele et al., 1992; Dlugokencky et al., 1994, 1995; Khalil and Rasmussen, 1984, 1987, 1988, 1990, 1994; Trivett et al., 1989; Novelli et al., 1992, 1994, 1998] and therefore little can be learned for these three compounds from our limited data set. Our results for carbon dioxide and methane show excellent agreement with the available published values (Table 5). The global trend for carbon monoxide is significantly smaller than that derived from our observations at Alert. Obviously, for compounds with atmospheric residence times of a few months or less trends derived from our observations at Alert are not representative on a global scale.

[23] The published data sets on seasonal cycles of VOC at midnorthern latitude and high northern latitude only cover time periods of 1 or 2 years and therefore are of limited value to determine representative, average seasonal cycles. Nevertheless, a comparison of the most prominent features, e.g., average summer and winter mixing ratios, seems justified (Table 6). In general, our summer and winter averages agree with most of the published average values. However, there are two data sets that differ significantly from our results. Except for ethane and the summer average mixing ratio of propane, all values reported by Lindskog and Moldanová [1994] are significantly higher than our averages. This is most likely the consequence of the impact of local or regional emissions since their sampling site was located close to major urban areas. In contrast to this, the values reported by Boudries et al. [1994] are at the lower

GAUTROIS ET AL.: VOC IN THE LOWER POLAR TROPOSPHERE

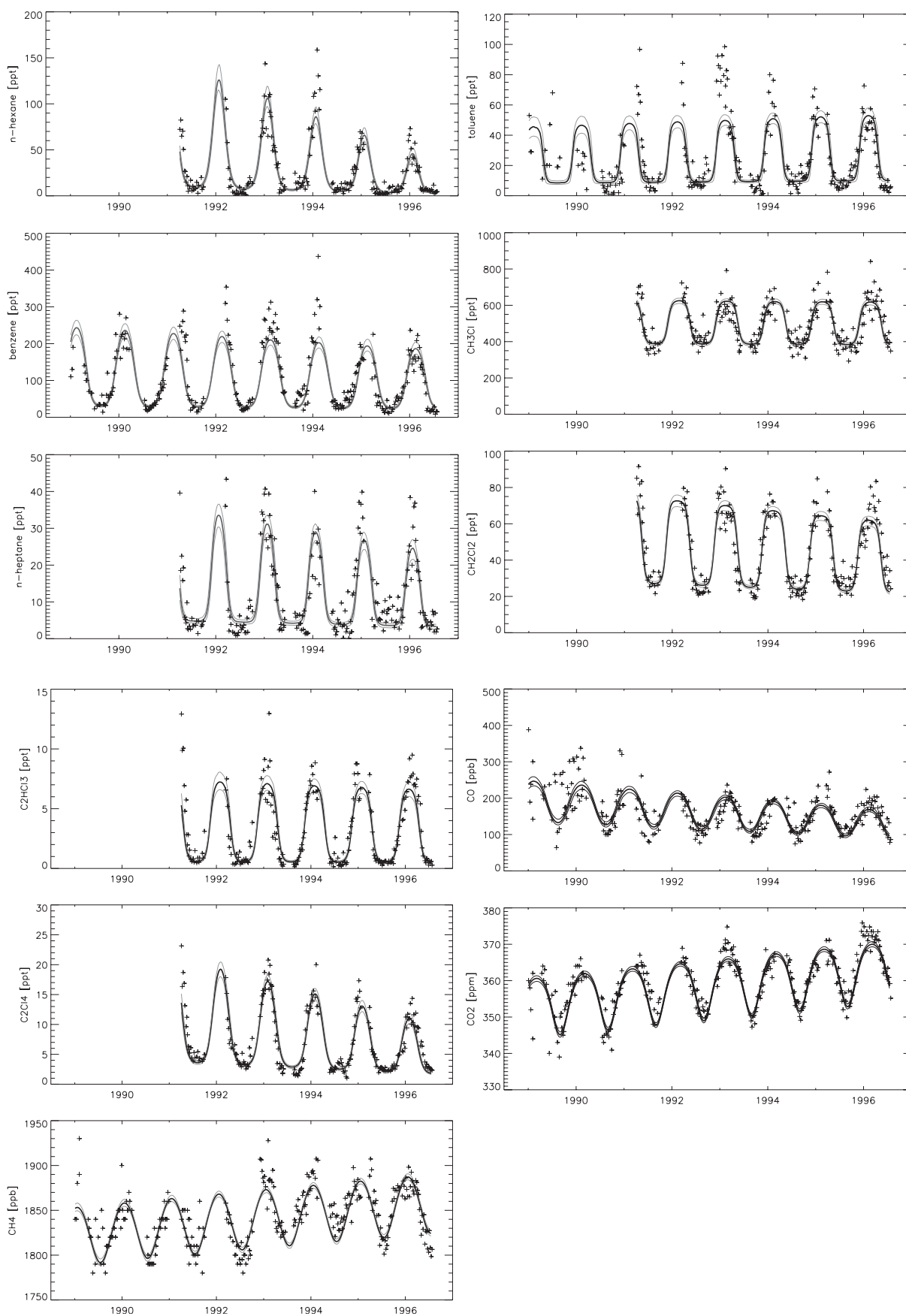


Figure 2. (continued)

**Table 3.** Parameters Derived From the Fit of Observed Mixing Ratios to Equation (2)

	$C_0$ , ppt	$\alpha$ , % yr <sup>-1</sup>	$\Phi$	$\beta$	$C_1$	$C_2$
Ethyne	239.0	1.60	5.59	0.93	-0.69	1.03
Ethane	1684.1	-3.31	5.50	1.00	-4.68	0.31
Propane	654.3	-0.61	5.68	1.00	-5.64	0.50
<i>i</i> -Butane	137.2	-8.22	5.68	1.00	-5.81	0.36
<i>n</i> -Butane	275.3	-9.57	5.83	1.00	-5.45	0.37
<i>n</i> -Pentane	85.5	-16.59	5.83	1.01	-0.99	0.89
<i>n</i> -Hexane	29.9	-22.90	5.87	0.98	-1.85	1.04
Benzene	101.6	-3.75	5.48	0.86	-0.57	1.19
<i>n</i> -Heptane	11.8	-7.97	5.88	0.80	-1.26	1.90
Toluene	25.8	2.52	5.64	0.70	-0.93	2.41
Methyl chloride	493.7	-0.37	5.40	0.24	-0.23	1.93
Dichloromethane	45.4	-4.04	5.53	0.48	-0.04	2.12
Trichloroethene	3.2	-2.79	5.78	0.88	-0.43	1.74
Tetrachloroethene	7.3	-13.52	5.71	0.80	-0.80	1.16
Methane	$1.84 \times 10^6$	0.25	5.99	10.6	1.49	0.09
Carbon monoxide	$153 \times 10^3$	-5.72	5.53	0.48	0.19	0.75
Carbon dioxide	$361.8 \times 10^6$	0.37	5.23	7170	2.22	0.43

end of the range of our data. Especially, their winter values are significantly lower than nearly all other wintertime observations. Since their measurements were made at the southernmost of the locations included in Table 6, this

might be interpreted as an indication for a latitudinal gradient of VOC mixing ratios. Indeed, the results of Rudolph [1995] show a strong, systematic latitudinal gradient of the wintertime ethane mixing ratios at midnorthern latitude and high northern latitude. The summertime gradient derived by Rudolph is very weak, compatible with the better agreement of the summertime mixing ratios reported by Boudries et al. with other data sets. However, the spatial and temporal coverage of the available data sets is too limited to allow firm, general conclusions.

[24] It should be noted that the mixing ratios reported for the least reactive VOC generally differ by less than 10–20% whereas the highly reactive VOC often vary by a factor of 2 or more between the individual measurement series. This most likely reflects the more pronounced impact of local or regional sources on mixing ratios of short-lived trace gases. But also the generally higher variability of the mixing ratios of highly reactive trace gases might contribute in the case of data sets with limited temporal coverage.

### 3.4. Secular Mixing Ratio Trends

[25] Obviously, the available data set is not yet sufficient to develop a truly representative climatology of NMHC and

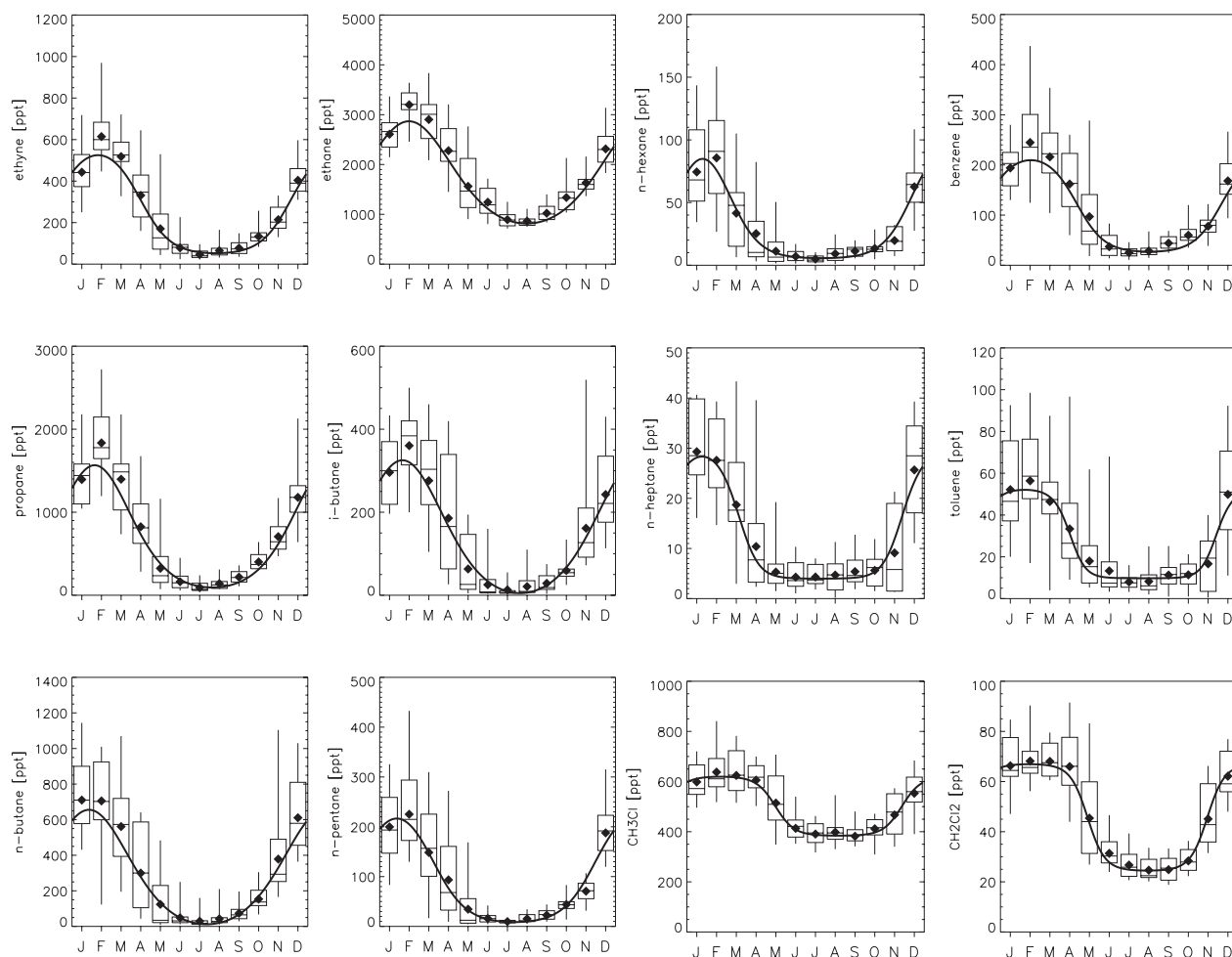


**Figure 3.** Annual cycle of organic compounds at Alert during 1989–1996. The symbols denote monthly binned data (blue diamonds, mean monthly mixing ratio; red, 5, 25, 50, 75, and 95% percentiles). The line represents the periodic part of the fit function (equation (2), linear term trend removed). (See color version of this figure in the HTML.)

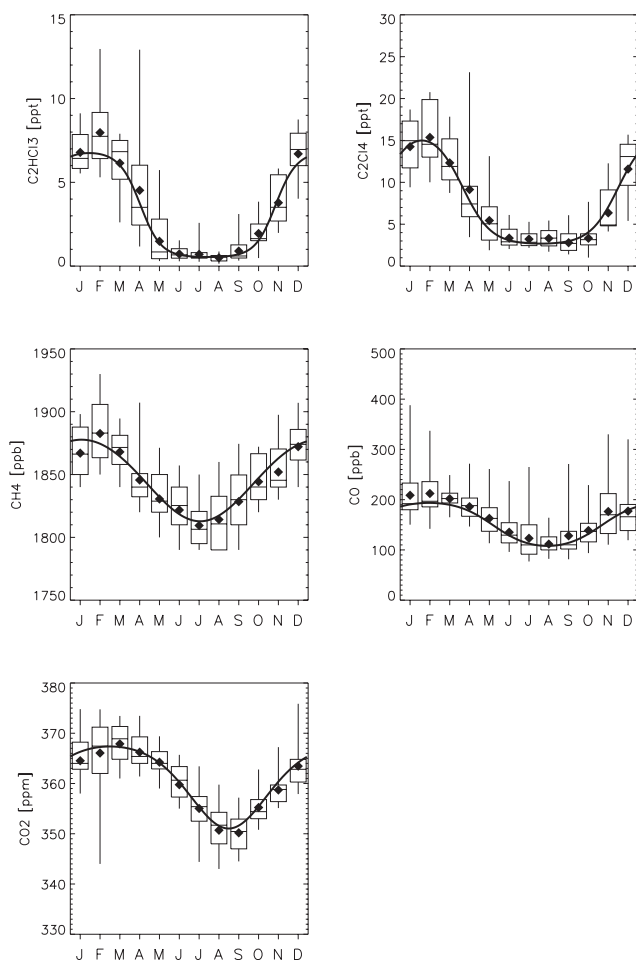


Figure 3. (continued)

chlorocarbons concentrations at Alert. Nevertheless, a 7-year observation period is qualified to study the possibility of systematic trends and to look for possible changes that might have occurred during this period.

**Table 4.** Result of Bootstrap Analysis of Uncertainties of the Trend Parameter  $\alpha$  in Equation (2)

	Least Squares Fit, % yr <sup>-1</sup>	Average Bootstrap Analysis, % yr <sup>-1</sup>	Standard Deviation From Bootstrap Analysis, % yr <sup>-1</sup>
Ethyne	1.60	1.61	1.22
Ethane	-3.31	-3.40	0.519
Propane	-0.607	-0.638	1.21
<i>i</i> -Butane	-8.22	-8.27	1.54
<i>n</i> -Butane	-9.57	-9.55	1.60
<i>n</i> -Pentane	-16.6	-16.8	2.40
<i>n</i> -Hexane	-22.9	-22.9	2.34
Benzene	-3.75	-3.83	1.34
<i>n</i> -Heptane	-7.97	-7.86	3.05
Toluene	2.52	2.33	2.04
Methyl chloride	-0.367	-0.324	0.714
Dichloromethane	-4.04	-4.15	1.02
Trichloroethene	-2.79	-2.65	2.76
Tetrachloroethene	-13.5	-13.5	1.27
Methane	0.254	0.257	0.0284
Carbon monoxide	-5.72	-5.71	0.783
Carbon dioxide	0.366	0.364	0.0278

**Table 5.** Comparison of Observed Trends of Mixing Ratios With Literature Data

Compound	Trend	Relative Trend	Literature
Methane	$+4.8 \pm 0.5$ ppb yr <sup>-1</sup>	+0.25%	+4 to +10 ppb yr <sup>-1</sup> <sup>a,b</sup> 0.65% <sup>c</sup>
Carbon monoxide	$-8.8 \pm 1.2$ ppb yr <sup>-1</sup>	-5.72%	-2.0 to -2.7 ppb yr <sup>-1</sup> <sup>c</sup> $-0.8 \pm 1.2$ % <sup>d</sup>
Carbon dioxide	$+1.3 \pm 0.1$ ppm yr <sup>-1</sup>	+0.37%	+1.5 ppm yr <sup>-1</sup> <sup>e</sup>

<sup>a</sup>Ehhalt [1999].

<sup>b</sup>Dlugokencky et al. [1994].

<sup>c</sup>Novelli et al. [1998].

<sup>d</sup>Zander et al. [1989].

<sup>e</sup>Trivett et al. [1989].

[26] There are several ways to calculate an average trend. Due to the very substantial seasonal variation of concentrations observed for most of the substances results can be somewhat different if the trends depend on season. The average change rates calculated by four different methods are listed in Table 7. One method is based on the fit procedure to a combination of a periodic function and a linear trend as described above. The second method, which uses a fit to the same function but a bootstrap procedure to determine the statistical uncertainty of the derived trend, has also been described previously. The other two are linear regressions of the data for each month of the year versus the year. In other words, individual rates of change are calculated from all measurements made in January, February, etc. This avoids bias resulting from the substantial seasonal variations and the not necessarily random selection of the measurement periods. Since the number of data points per month is very small, the uncertainty of these change rates often is substantial. To reduce random variability the change rates for the individual months are combined to an annual average. This is done for the absolute and the relative increase rates (ratio of trend for a given month of the year over the monthly mean mixing ratio). Thus both procedures give different weights to the different months, depending on the monthly means of the mixing ratios. Although none of the differences between the results from different procedures are significant on a  $2\sigma$  significance level, for ethyne, propane, the butanes, and trichloroethene the results differ on a  $1\sigma$  significance level. This is an indication for a seasonal dependence of the trend. Indeed, for NMHC the largest relative decrease rates are found for late spring and summer, whereas the relative trend observed for fall and winter is nearly always close to zero. The only exception is ethyne where the rates of change are very close to zero for all 12 months of the year. However, due to the limited number of data points for each month, these differences are generally only significant at a  $1\sigma$  level. Nevertheless, the consistent finding of higher relative decrease rates in summer indicates this summer/winter difference in secular trends for NMHC is most likely systematic. No indication for such a systematic difference in trends between seasons could be found for the chlorocarbons.

[27] For a substantial number of components the annual average change rates are consistently different from zero at a  $1\sigma$  confidence level, for few components the significance level exceeds  $2\sigma$ , but only for tetrachloroethene, ethane, *i*-butane, *n*-butane, and *n*-hexane the trends are

**Table 6.** Comparison of Average Summer and Winter Nonmethane Hydrocarbons Mixing Ratios Reported for Different Locations at Midnorthern Latitude and High Northern Latitude<sup>a</sup>

	Boudries <i>et al.</i> [1994], France, Poissopder (48°N, 4°W)		Jobson <i>et al.</i> [1994], Canada, Fraserdale (50°N, 82°W)		Lindskog and Moldanova [1994], Sweden, Rörvik (57°N, 12°E)		Penkett <i>et al.</i> [1993], North Atlantic		Laurila and Hakola [1996], Norway, Pallas (68°N, 24°E)		This Work, Canada, Alert (82°N, 62°W)	
	Winter <sup>b</sup>	Summer	Winter <sup>c</sup>	Summer <sup>d</sup>	Winter	Summer	Winter	Summer	Winter	Summer	Winter	Summer
Ethane	1550	730	2450	820	2520	850	2220	1210	2215	780	2702 ± 492	1008 ± 233
Ethylene	415	73	820	75	1140	205	673	126	710	100	483 ± 131	67 ± 37
Propane	695	110	1440	78	1270	240	870	85	1200	140	1422 ± 413	158 ± 87
<i>i</i> -Butane	130	49	310	7	467	155	193	47	234	17	288 ± 101	23 ± 27
<i>n</i> -Butane	240	45	620	15	830	255	405	25	463	45	647 ± 218	50 ± 47
<i>n</i> -Pentane	74	18	230	13	391	108	147	8	152	25	189 ± 75	16 ± 10
<i>n</i> -Hexane	22	10					65	5	54	3	65 ± 33	8 ± 5
Benzene	53	30					230	25	210	28	201 ± 63	34 ± 17
Toluene	170	85					115	10			51 ± 22	10 ± 9

<sup>a</sup>Unless otherwise indicated, summer is defined as June to September, and winter is defined as December to March. Values are given in ppt.

<sup>b</sup>December and January.

<sup>c</sup>January and February.

<sup>d</sup>June to August.

significant on a  $3\sigma$  confidence level. Since our data cover only a limited number of years, and the data exhibit a considerable interannual variability, the trend parameters cannot be interpreted as a regular and constant, annual change rate. However, they are very strong indicators for significant changes occurring during our observation period.

[28] Variations in atmospheric transport patterns can cause very significant changes in the atmospheric mixing ratios of reactive trace gases. However, this generally results in interannual variability, a systematic trend in tropospheric transport over a 7-year period, which would be sufficient to cause the observed substantial trends in NMHC mixing ratios seem unlikely. Similarly, an increase in the tropospheric OH-radical concentrations can cause a decrease in NMHC mixing ratios. However, although it is possible that the tropospheric OH-radical concentration changes as a consequence of changes in the mixing ratios of important atmospheric trace gases, the expected rates of change [Krol *et al.*, 1998; Spivakovsky *et al.*, 2000; Prather and Ehhalt, 2001; Prinn *et al.*, 2001] are much lower than the changes in NMHC mixing ratios we found.

[29] Another possibility is the decrease in emission rates. Although to our knowledge there are no direct data on the temporal development of the global emissions of NMHC, there is information on trace gases with significant emissions for source types similar to that of NMHC. Novelli *et al.* [1998] reported a decrease of the tropospheric mixing ratio of carbon monoxide for the period between 1990 and 1996, and mentioned a decrease in emission rates as the likely explanation. There are also reports of declining carbon monoxide emission rates from sources in industrialized countries [U.S. Environmental Protection Agency, 1998; Mylona, 2000].

[30] Similarly, for dichloromethane and tetrachloroethene there are reports that man-made emissions decreased between 1988 and 1996 [McCulloch *et al.*, 1999]. The emissions of tetrachloroethene changed drastically from 0.42 Tg yr<sup>-1</sup> in 1988 to 0.24 Tg yr<sup>-1</sup> in 1996, the reduction in dichloromethane emissions was somewhat less pronounced, it changed from 0.59 Tg yr<sup>-1</sup> in 1988 to 0.48 Tg yr<sup>-1</sup> in 1996. These emission reductions are fully compatible with trends we observed at Alert. In total we therefore believe that decreases in emissions is the main, although not necessarily the only factor, which has been driving the observed decrease in NMHC and chlorocarbon mixing ratios at Alert.

### 3.5. Seasonal Cycles

[31] The time series in Figure 2 exhibit clear periodic seasonal cycles for all compounds studied. There is substantial scatter of the data and also some interannual variability. Nevertheless, since our record covers 7 years for most of the studied substances, averaged seasonal cycles will be reasonably representative. Monthly averages for the whole period are shown in Figure 3. On average, there are more than 20 data points for each month of the year; the difference in the number of samples between different months does not exceed the uncertainty expected for a random process ( $21 \pm 4$  measurements per month). Table 8 summarizes the annual means, medians, maximum, and minimum mixing ratios of the average seasonal cycles together with their uncertainties.

**Table 7.** Trend of Volatile Organic Compounds Mixing Ratios at Alert for the Period From 1989 to 1996<sup>a</sup>

Compound	C <sub>0</sub> , ppt	Fit According to Equation (2)		Bootstrap		Average of Absolute Monthly Change Rates		Average of Relative Monthly Change Rates	
		% yr <sup>-1</sup>	ppt yr <sup>-1</sup>	% yr <sup>-1</sup>	ppt yr <sup>-1</sup>	% yr <sup>-1</sup>	ppt yr <sup>-1</sup>	% yr <sup>-1</sup>	ppt yr <sup>-1</sup>
Methyl chloride <sup>b</sup>	494	-0.37	-1.8	-0.32 ± 0.71	-1.6 ± 3.5	-1.4 ± 1.5	-7.0 ± 7.3	-1.6 ± 1.5	-8.2 ± 7.5
Dichloromethane <sup>b</sup>	45.4	-4.0	-1.8	-4.2 ± 1.0	-1.9 ± 0.5	-3.2 ± 1.9	-1.5 ± 0.9	-2.8 ± 1.9	-1.3 ± 0.9
Tetrachloroethene <sup>b</sup>	7.3	-13.5	-1.0	-13.5 ± 1.3	-1.0 ± 0.1	-15.0 ± 2.9	-1.1 ± 0.22	-15.8 ± 1.5	-1.2 ± 0.1
Ethane	1684	-3.3	-55.6	-3.4 ± 0.5	-57.3 ± 8.4	-3.6 ± 0.9	-65.7 ± 16.9	-3.6 ± 0.8	-66.0 ± 13.8
Ethyne	239	1.60	3.8	1.6 ± 1.2	3.8 ± 2.9	0.2 ± 1.3	1.0 ± 3.3	-0.9 ± 1.6	-2.2 ± 4.1
Propane	654	-0.6	-3.9	-0.64 ± 1.2	-4.2 ± 0.8	-1.9 ± 1.8	-16.7 ± 12.5	-5.0 ± 2.5	-35.8 ± 17.9
Benzene	102	-3.8	-3.9	-3.8 ± 1.3	-3.9 ± 1.3	-3.6 ± 2.2	-4.8 ± 2.3	-4.5 ± 2.6	-5.0 ± 2.9
<i>i</i> -Butane	137	-8.2	-11.2	-8.3 ± 1.5	-11.4 ± 2.1	-10.3 ± 2.3	-14.9 ± 3.3	-16.4 ± 3.4	-23.6 ± 4.9
<i>n</i> -Butane	275	-9.6	-26.4	-9.6 ± 1.6	-26.4 ± 4.4	-12.2 ± 2.9	-37.5 ± 9.0	-18.3 ± 3.6	-56.0 ± 10.9
Trichloroethene	3.2	-2.8	-0.1	-2.6 ± 2.8	-0.1 ± 0.1	-6.3 ± 2.7	-0.2 ± 0.1	-10.7 ± 3.6	-0.4 ± 0.1
<i>n</i> -Pentane <sup>b</sup>	85.5	-16.6	-14.2	-16.8 ± 2.4	-14.4 ± 2.1	-14.4 ± 5.0	-12.7 ± 4.4	-13.1 ± 5.5	-11.6 ± 4.9
<i>n</i> -Hexane <sup>b</sup>	30	-22.9	-6.9	-22.9 ± 2.3	-6.9 ± 0.7	-19.2 ± 7.7	-6.5 ± 2.3	-17.3 ± 5.0	-5.2 ± 1.5
Toluene	25.8	2.5	0.6	2.3 ± 2.0	0.6 ± 0.5	0.8 ± 3.1	0.3 ± 0.9	-2.8 ± 4.5	-0.8 ± 1.4
<i>n</i> -Heptane <sup>b</sup>	11.8	-8.0	-0.9	-7.9 ± 3.1	-0.9 ± 0.4	-1.1 ± 7.3	-0.3 ± 0.7	2.5 ± 9.3	0.3 ± 0.8

<sup>a</sup>Results from different calculation procedures are compared.

<sup>b</sup>Based on data from 1991 to 1996.

[32] There are several features that all seasonal cycles have in common. The mixing ratios maximize in spring and have a minimum in summer or early fall. For nearly all substances the summer minimum is rather broad, which combined with the random variability prevents the precise determination of the period with the lowest mixing ratio. In contrast to this, the occurrence of the wintertime maximum is clearly visible for most compounds and in general well defined within a window of about 2 weeks. Exceptions are methyl chloride and dichloromethane. These are, apart from methane, the least reactive substances we studied. Although it is evident that both compounds exhibit the highest mixing ratios between January and early April, the exact occurrence of the seasonal maximum is somewhat uncertain. For the more reactive chlorocarbons, tetrachloroethene, and trichloroethene, the seasonal maximum is better defined, although still with a slightly higher uncertainty than for the NMHC.

[33] The results indicate a systematic dependence between the time of the occurrence of the maximum and the reactivity of the compounds.

[34] Qualitatively the dependence between rate constant and the main characteristics of the shape of the seasonal cycle can be explained by the seasonal variability of the OH-radical concentration. However, quantitatively the results demonstrate a complex interaction between transport and atmospheric loss mechanisms. At the time of the occurrence of the NMHC concentration maxima, the OH-radical concentration at the latitude of Alert is effectively zero [Spivakovsky *et al.*, 2000]. Similarly, the relative decrease rates require OH-radical concentrations that cannot be explained by the OH-radical concentrations at the latitude of Alert. Obviously, exchange with lower latitudes plays a major role in determining the wintertime maxima. Indeed, north of 45°N even for the most reactive of the studied NMHC (toluene, hexane, and pentane) the atmospheric lifetime during the occurrence of their maximum exceeds 1 month. This is more than sufficient to allow effective transport from latitudes with high emission rates of NMHC. However, for summer we calculate from the reaction rate constants and the OH-radical concentration

**Table 8.** Summary of Median, Average, Maximum, and Minimum Mixing Ratios for the Average Seasonal Cycles of Several Nonmethane Hydrocarbons and Halocarbons at Alert

Compound	OH Rate Constant × 10 <sup>14</sup> , mol cm <sup>-3</sup> s <sup>-1a</sup>	Median, ppt	Average, ppt	Maximum, ppt	Minimum, ppt
Carbon dioxide		360	360 ± 8	365 ± 6	354 ± 6
Methane		1843	1845 ± 30	1873 ± 20	1822 ± 22
Carbon monoxide		157	163 ± 56	198 ± 53	127 ± 44
Methyl chloride	3.17	497	500 ± 15	636 ± 18	384 ± 8
Dichloromethane	10.1	45.8	47.2 ± 2	71.6 ± 1.9	24.2 ± 0.9
Tetrachloroethene	12.9	7.2	7.6 ± 0.6	15.3 ± 0.9	2.7 ± 0.4
Ethane	20.1	1800	1813 ± 70	3245 ± 74	832 ± 28
Ethyne	74.0	243	256 ± 18	586 ± 24	44 ± 4
Propane	97.7	695	714 ± 52	1807 ± 83	93 ± 13
Benzene	114	107	112 ± 9	244 ± 14	23 ± 2
<i>i</i> -Butane	203	131	144 ± 16	345 ± 18	14 ± 3
<i>n</i> -Butane	222	285	306 ± 34	732 ± 45	26 ± 5
Trichloroethene	245	3.3	3.5 ± 0.3	7.8 ± 0.5	0.5 ± 0.1
<i>n</i> -Pentane	368	83	89 ± 11	239 ± 28	8 ± 1
<i>n</i> -Hexane	526	28.2	30.3 ± 4.2	82 ± 10	4.5 ± 0.7
Toluene	663	25.6	29.8 ± 3.5	59.5 ± 7.3	6.1 ± 1
<i>n</i> -Heptane	687	11.7	12.5 ± 1.4	31.1 ± 1.9	3.8 ± 0.5

<sup>a</sup>Rate constants are taken from Atkinson [1986] and Atkinson *et al.* [1997a, 1997b]. Rate constants are given for 280 K if temperature dependence is known.

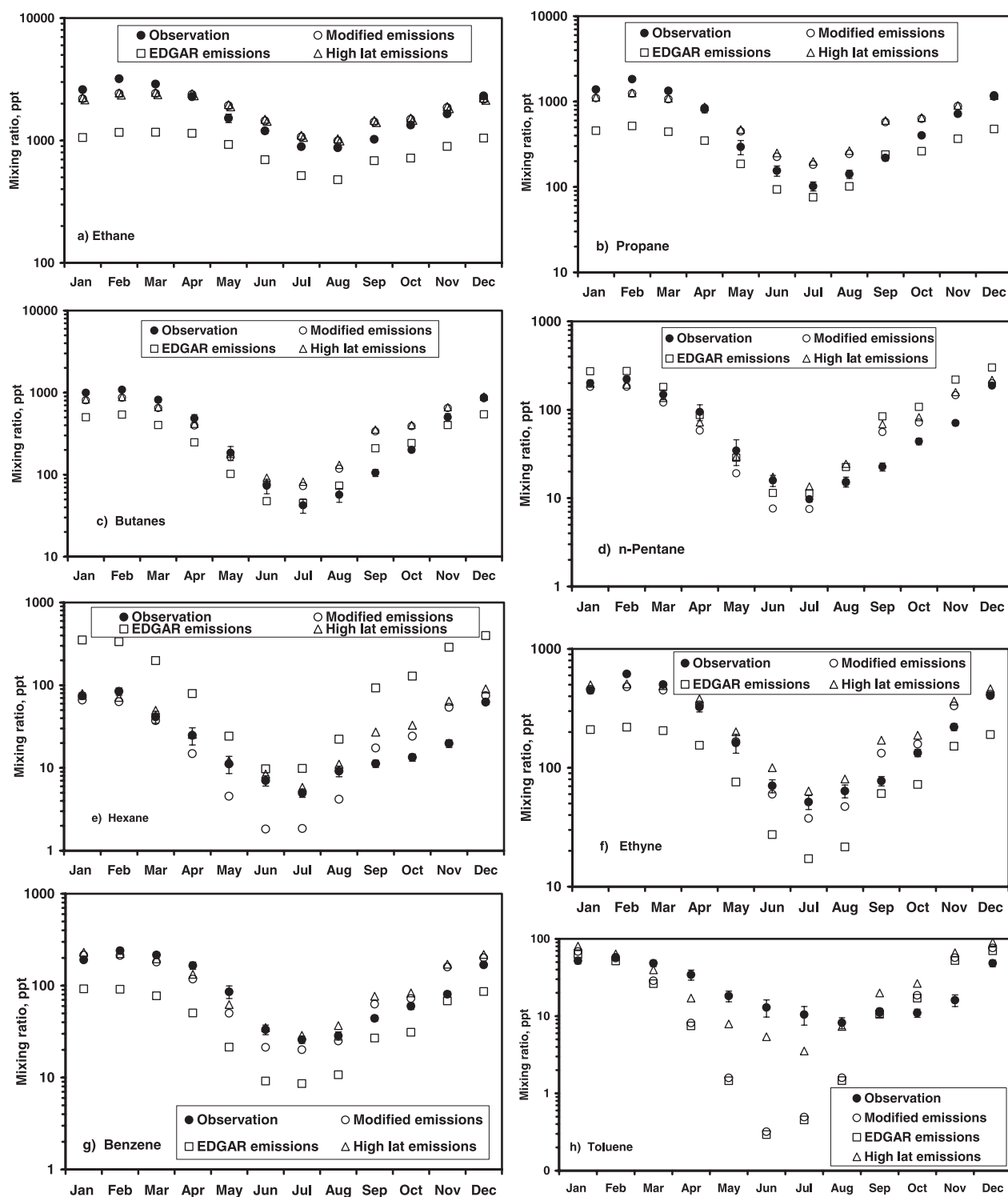


**Figure 4.** (a–h) Comparison of measured (solid circles) and modeled (squares) monthly mean nonmethane hydrocarbons (NMHC) mixing ratios at Alert. The open squares represent model results based on the Emission Database for Global Atmospheric Research (EDGAR) emission inventory; the open circles are based on emission rates scaled to generate the observed annual mean NMHC mixing ratios. Shown are also model results including an additional high latitude emission of  $0.03 \text{ Tg yr}^{-1}$  (triangles).

**Table 9.** Emission Inventories of Nonmethane Hydrocarbons From Different Sources for 1990 (Based on the Emission Database for Global Atmospheric Research Database)

Source	Emission Rates of Nonmethane Hydrocarbons in kg compound yr <sup>-1</sup>							
	Ethane	Ethyne	Propane	Butanes	Pentanes	Hexanes and Heavier Alkanes	Benzene	Toluene
Use and burning of fossil fuel								
Industry	$8.52 \times 10^6$	$4.26 \times 10^6$	$1.96 \times 10^7$	$4.81 \times 10^7$	$5.21 \times 10^7$	$8.92 \times 10^7$	$1.97 \times 10^7$	$4.10 \times 10^7$
Power plants	$1.81 \times 10^6$	$9.11 \times 10^5$	$7.62 \times 10^6$	$1.92 \times 10^7$	$2.47 \times 10^7$	$2.25 \times 10^7$	$7.65 \times 10^6$	$1.11 \times 10^7$
Refineries	$2.51 \times 10^8$	$2.96 \times 10^6$	$8.88 \times 10^8$	$8.87 \times 10^8$	$1.11 \times 10^9$	$8.87 \times 10^8$	$1.03 \times 10^8$	$1.35 \times 10^8$
Domestic use (heating, cooking, etc.)	$1.51 \times 10^8$	$5.26 \times 10^7$	$1.21 \times 10^8$	$9.60 \times 10^7$	$8.12 \times 10^7$	$1.21 \times 10^7$	$7.44 \times 10^7$	$2.32 \times 10^7$
Transport: road traffic	$3.04 \times 10^8$	$9.88 \times 10^8$	$1.94 \times 10^8$	$4.37 \times 10^9$	$5.65 \times 10^9$	$6.88 \times 10^9$	$1.05 \times 10^9$	$2.51 \times 10^9$
Transport: rail and ship	$9.33 \times 10^6$	$2.14 \times 10^7$	$4.93 \times 10^6$	$2.84 \times 10^7$	$3.14 \times 10^7$	$1.25 \times 10^8$	$2.08 \times 10^7$	$4.86 \times 10^7$
Transport: aircraft	$4.45 \times 10^5$	$2.11 \times 10^6$	$9.10 \times 10^4$		$1.06 \times 10^5$	$2.66 \times 10^6$	$9.81 \times 10^5$	$2.63 \times 10^5$
Oil production	$1.36 \times 10^9$		$4.25 \times 10^9$	$6.87 \times 10^9$	$3.89 \times 10^9$	$6.22 \times 10^9$	$2.26 \times 10^7$	
Gas production	$1.84 \times 10^9$		$6.21 \times 10^8$	$7.12 \times 10^8$	$1.60 \times 10^8$	$7.20 \times 10^7$		
Use and burning of biomass								
Industry	$4.45 \times 10^7$	$2.87 \times 10^7$	$1.50 \times 10^7$	$3.03 \times 10^6$	$6.66 \times 10^6$	$6.06 \times 10^6$	$4.12 \times 10^7$	$1.82 \times 10^7$
Domestic use (heating, cooking, etc.)	$1.79 \times 10^9$	$1.21 \times 10^9$	$5.69 \times 10^8$	$1.33 \times 10^8$	$2.92 \times 10^8$	$2.66 \times 10^8$	$1.81 \times 10^9$	$7.97 \times 10^8$
Industrial processes								
Chemicals	$7.81 \times 10^6$		$5.33 \times 10^6$	$3.60 \times 10^6$	$1.70 \times 10^6$		$4.42 \times 10^5$	$1.05 \times 10^5$
Solvents						$7.13 \times 10^9$		$1.71 \times 10^9$
Agriculture								
Deforestation and harvesting practices	$1.18 \times 10^9$	$8.74 \times 10^8$	$3.25 \times 10^8$	$1.02 \times 10^8$	$2.24 \times 10^8$	$2.03 \times 10^8$	$1.38 \times 10^9$	$6.10 \times 10^8$
Waste management	$1.27 \times 10^9$	$8.18 \times 10^8$	$6.05 \times 10^8$	$7.85 \times 10^8$	$7.94 \times 10^8$	$1.31 \times 10^9$	$1.28 \times 10^9$	$7.69 \times 10^8$
Sum	$8.22 \times 10^9$	$4.01 \times 10^9$	$7.63 \times 10^9$	$14.1 \times 10^9$	$12.3 \times 10^9$	$23.2 \times 10^9$	$5.80 \times 10^9$	$6.67 \times 10^9$

that the atmospheric lifetime of the most reactive NMHC is about 1 week at the latitude of Alert and less than 1 day south of 60°N. For the less reactive NMHC such as ethane, benzene, and propane during summer the lifetime for the latitude of Alert is still in the range of months, but decreases rapidly with decreasing latitude. Clearly, the footprint area for the studied NMHC and chlorocarbons depends not only on atmospheric transport and OH reactivity, but also on season.

#### 4. Comparison With Model Calculations

[35] In order to gain more detailed insight into the factors determining the concentrations of NMHC at Alert, we conducted numerical model simulations. In Figure 4 the observed seasonal cycles are compared with the results of model calculations. The model calculations are performed with the Harvard/GISS/University of California, Irvine Chemical Tracer Model (CTM) described by *Prather et al.* [1987]. Meteorological parameters such as wind speed, pressure, temperature, and dry and wet convection fluxes were adopted from the GISS Global Circulation Model (GCM II) [*Hansen et al.*, 1983] with a time resolution of 6 hours. In the present study the horizontal resolution was 4° in latitude and 5° in longitude. The vertical resolution was nine levels up to 10 hPa, seven of them located in the troposphere. The chemical system of the CTM was kept as simple as possible. Each NMHC was treated separately allowing only emission and transport of a single NMHC during each run. The chemistry of this NMHC was described by its reaction with OH radicals using reaction parameters given by *Atkinson* [1986] and *Atkinson et al.* [1997a, 1997b]. The global field of OH was prescribed using three-dimensional monthly means provided by *Spivakovsky et al.* [2000].

[36] The NMHC emission rates for the model calculations were taken from the Emission Database for Global Atmospheric Research (EDGAR), which was established by TNO (Netherlands Organization for Health and Environment) and RIVM (National Institute for Public Health and the Environment, Netherlands) [*Olivier et al.*, 1996]. Oceanic emissions and vegetation sources are neglected which might result in a systematic underestimate of the NMHC source strength. However, biogenic emissions of the substances studied here are generally small [*Rudolph*, 1995, 1996] and consequently such a bias should be negligible compared to the man-made emissions included in the EDGAR database (Table 9).

[37] The results of the model calculations strongly depend on the transport field, the OH-radical concentrations, the rate constant and its temperature dependence for the reaction of the studied NMHC with OH, and the source strength and source distribution. *Spivakovsky et al.* [2000] estimates the uncertainty in the OH radical concentration field to be 10–15% and the uncertainty in the rate constants and their temperature dependence are typically in the range of 15–30% [*Atkinson*, 1986; *Atkinson et al.*, 1997a, 1997b]. The consequences of uncertainty in transport or emission distributions are difficult to quantify. Nevertheless, in general the model calculations give a reasonable description of some of the relative features of the measured seasonal variability, e.g., time of the occurrence of the maxima and minima (Figure 4). However, for most compounds the model results are systematically lower than the observations. To some extent this can be explained by an underestimate of the emission rates in the model. For example, the EDGAR emission inventory gives a global ethane emission rate of 8.2 Tg yr<sup>-1</sup>, only about half the emission rate required to balance the atmospheric budget, which was derived by *Rudolph* [1995] from atmospheric observations.

**Table 10.** Comparison of Global Annual Emission Rates According to the Emission Database for Global Atmospheric Research (EDGAR) Emission Inventory and the Emission Rates Modified to Generate Optimum Agreement for Annual Average Mixing Ratios Modeled and Observed at Alert

Compound	EDGAR Emissions, Tg yr <sup>-1</sup>	Modified Emissions, Tg yr <sup>-1</sup>
Ethane	8.2	17.1
Propane	7.6	18.4
<i>n</i> + <i>i</i> -Butane	14.1	22.7
<i>n</i> -Pentane	12.4 <sup>a</sup>	8.2
<i>n</i> -Hexane	23.3 <sup>b</sup>	4.4
Ethyne	4.0	8.8
Benzene	5.8	13.6
Toluene	6.7	7.3

<sup>a</sup>EDGAR emission inventory for sum of all pentanes.

<sup>b</sup>EDGAR emission inventory for sum of all hexanes and heavier alkanes.

It should be noted that the impact of emissions at mid-latitude and low latitude strongly depends on the atmospheric lifetime of the studied compound (see below), and emissions in the Southern Hemisphere only have a marginal

impact on the atmospheric mixing ratios of NMHC at Alert. Nevertheless, increasing the emission rates in the model by a factor that is independent of latitude or longitude reduces the discrepancy between observations and model (Figure 4). In Table 10 the NMHC emission rates based on the EDGAR emission inventory and the modified emission rates are compared. For ethane, propane, the butanes, and benzene the factor is approximately 2. It should be noted that in the case of *n*-pentane and *n*-hexane a direct comparison is not possible. In the case of pentane the EDGAR database only gives emissions for the sum of all pentanes. However, a distribution between the different isomers can be made on the basis of the ratio of pentane emissions. McLaren *et al.* [1996] report that the ratio of *n*-pentane to *i*-pentane emissions from transportation related sources is 0.5. The emissions of the third pentane isomer are negligible. Based on the emission ratios of McLaren *et al.* the EDGAR database pentane emissions correspond to an *n*-pentane emission of 4.1 Tg yr<sup>-1</sup>, again a factor of 2 lower than the emission rates required for optimum agreement between modeling results and observations. The emission rates for

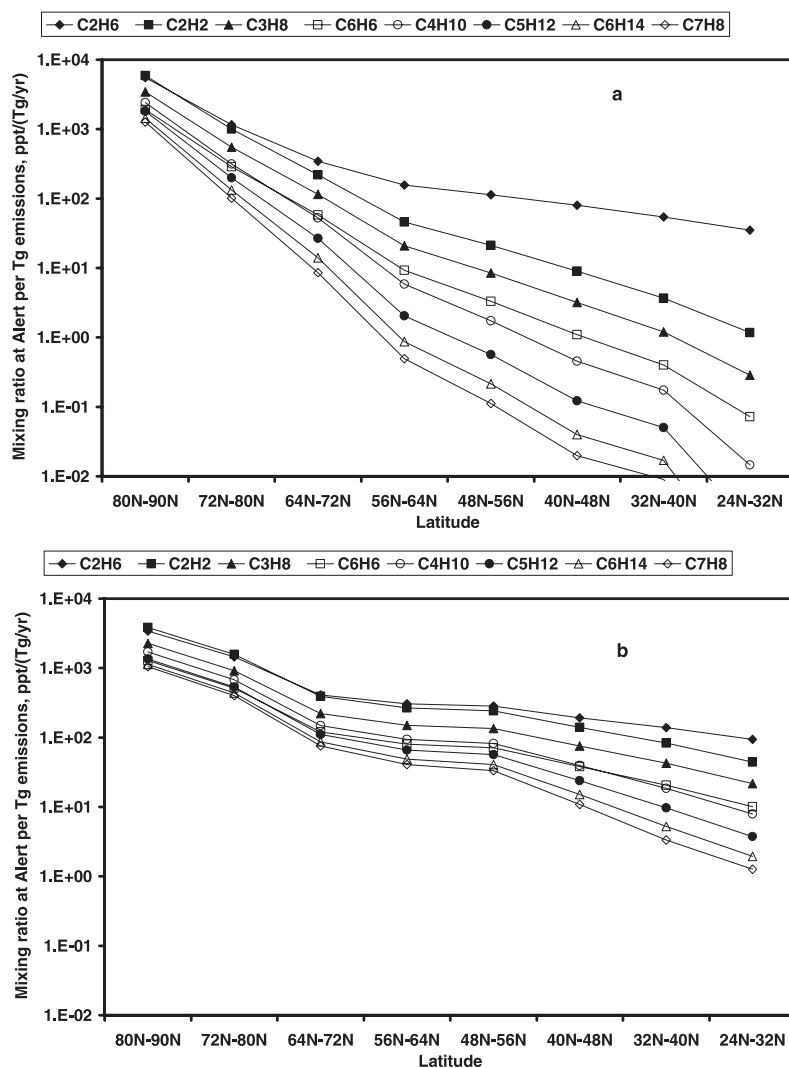


**Figure 5.** Modeled mixing ratios at Alert in (a) July and (b) January for an emission rate of 1 Tg yr<sup>-1</sup> in the specified latitude band.

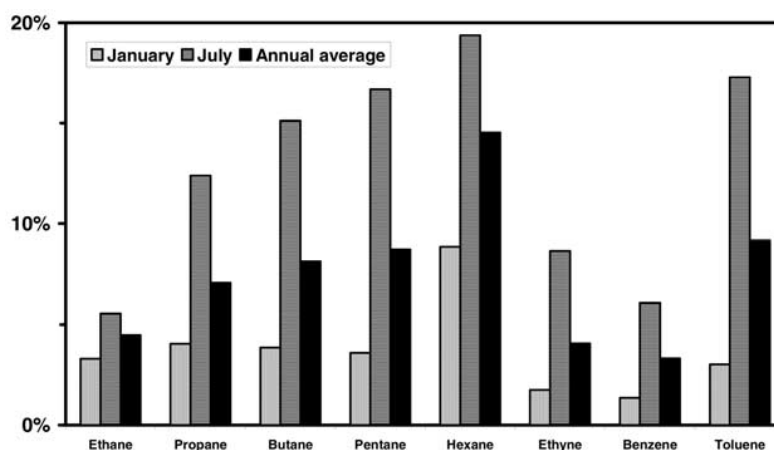


**Figure 6.** Relative decrease in hydrocarbon mixing ratios at Alert calculated for a 20% relative decrease in high latitude nonmethane hydrocarbons (NMHC) emissions.

hexane in the EDAGR database include all  $C_6$  and heavier alkanes, our results are for *n*-hexane only. It is therefore not surprising that the EDGAR emission rates are higher than the emission rates required to explain the observed *n*-hexane mixing ratios.

[38] For the less reactive NMHC (ethane, propane, ethyne, and benzene) uniformly increasing the emission rates in the model without changing the relative geographical or temporal distribution of the sources results in a reasonable, although not perfect, agreement between model and observations. For ethane and ethyne the differences between the model with adjusted emission rates and observations is on average less than 20%, for propane, butane, and benzene around 30%. As mentioned above, the mixing ratios at Alert are predominantly influenced by emissions from mid-northern latitude and high northern latitude and consequently the conclusions about required source strength are only valid for these latitudes.

[39] For the more reactive NMHC the agreement is less favorable. For hexane and toluene the average differences increase to more than 80% and a factor of 6.7, respectively. Moreover, for these compounds the model seriously overestimates the relative change in mixing ratios between summer and winter. With increasing reactivity of the studied NMHC the extent of the latitude range that has a visible impact on the NMHC mixing ratios decreases, especially in summer when the OH-radical concentrations have their maximum (Figure 5). Thus the substantial underestimation of the mixing ratios of reactive NMHC in summer points toward too low emission rates at higher latitudes in the model.

[40] In order to quantify the magnitude of the emission rates required to explain the discrepancy between model results and observations we conducted model calculations with NMHC emissions limited to bands of  $8^{\circ}$ – $10^{\circ}$  latitude. Within these latitude belts the relative spatial distribution of the sources was kept identical to that in the EDGAR database, outside of the latitude band all NMHC emissions were set to zero. The emission rates of each individual NMHC inside the specified latitude band was set to  $1 \text{ Tg yr}^{-1}$ . Figure 5 shows the calculated contribution of emissions from different latitude ranges on NMHC mixing ratios at Alert for January and July.

[41] These modeling results clearly predict that for reactive NMHC such as hexane and toluene during summer emissions at midlatitudes will not have any visible impact on the atmospheric mixing ratios at Alert. For example, an increase of toluene emissions of  $1 \text{ Tg yr}^{-1}$  in the latitude range of  $48^{\circ}$ – $56^{\circ}\text{N}$  will increase the toluene mixing ratios at Alert in July by about 0.1 ppt. The same increase in emission rates would increase the wintertime toluene mixing ratios at Alert by more than 30 ppt (Figure 5b).

[42] Based on the calculations shown in Figure 5, it is easy to determine the additional emission rates for different latitude bands, which would be required to explain the discrepancies between model results and observations.

[43] It is obvious that emissions, from below  $64^{\circ}$  northern latitude, are unlikely explanations for the summertime difference between measurements and model. First, this would require unidentified sources with emission rates of nearly  $100 \text{ Tg yr}^{-1}$ , orders of magnitude higher than the source strength of all identified sources together. Second, our model calculations predict that such high emission rates would result in wintertime mixing ratios of several hundred ppt, which is not compatible with the observations. Although a strong seasonal variability of the emission rates of such an unknown source cannot be ruled out, the existence of unidentified NMHC sources with emission rates in the range of  $100 \text{ Tg yr}^{-1}$  and a strong seasonal variability is extremely unlikely.

[44] A more plausible explanation is the existence of unaccounted emissions at high latitudes. The required emission rates are only a fraction of a  $\text{Tg yr}^{-1}$ , a small part of their total global emission rates. To study the impact of such a high latitude source, we added high latitude emissions of  $0.03 \text{ Tg yr}^{-1}$  to the “modified emissions” in our model calculations. The results are included in Figure 4. As can be seen, the addition of such a source drastically reduces the discrepancy between model and observations for the more reactive NMHC in summer, but has only a small impact on the mixing ratios of less reactive NMHC. Similarly, the resulting relative change in wintertime mixing ratios is marginal. Possible sources for such emissions are oil and natural gas exploitation in Alaska, Siberia, and northern Canada or boreal forest fires at high northern

latitudes. The dominance of high latitude emissions for the summertime mixing ratios of reactive NMHC at Alert has also an important consequence for the possible origin of the secular trend of the NMHC mixing ratios. Since the relative decrease rate of mixing ratios for many of the NMHC is more pronounced in summer than in winter, this strongly points toward a decrease of high latitude emissions. In Figure 6 the model predictions of the relative changes in NMHC mixing ratios at Alert resulting from a 20% decrease in high latitude NMHC emissions are presented. There is a strong impact on the summertime mixing ratios of reactive NMHC, whereas the predicted relative decrease for less reactive NMHC or during winter is significantly lower. This is fully compatible with our observations.

[45] *Dlugokencky et al.* [1994] mentioned that the drastic economic changes in the area of the former Soviet Union have resulted in a significant reduction of methane emissions due to reduction in fossil fuel exploitation and use for these regions, including Siberia. Since most of these methane sources are also sources for NMHC, it is plausible that the economic changes in the area of the Former Soviet Union resulted in reductions of NMHC emissions at high northern latitudes. The observed changes are most pronounced for saturated NMHC, which is fully compatible with reductions in emissions from oil and natural gas production. However, it has to be remembered that our results do not allow differentiating between reductions of emissions from the Former Soviet Union and other oil and gas producing high latitude regions such as Alaska, northern Canada, or Scandinavia.

## 5. Conclusions

[46] The differences in the relative shape of the seasonal cycles of the mixing ratios of individual NMHC or halocarbons at Alert systematically depend on their atmospheric residence times, specifically the reactivity toward the OH-radical. The systematic dependence between key descriptors of the shape of the seasonal cycles, such as the occurrence of maximum concentrations or relative amplitude of the seasonal cycle, and the rate constant for reaction with OH-radicals is fully consistent with the concept that the response of atmospheric concentrations to the seasonal variations in OH-radical concentration is faster for compounds with higher reactivity. The very low summertime values for reactive compounds are consistent with the short residence times in summer and the remoteness of the sampling location. However, the comparison between model calculations and observations also strongly suggests the existence of emissions from high latitude sources.

[47] The numerical model simulations describe several of the most prominent features of the observed seasonal cycles, but they fail in two important aspects. First, the modeled concentrations are in many cases significantly lower than the observations. This discrepancy points toward an underestimation of the sources in the model by approximately a factor of 2. Second, for the more reactive compounds the model calculations consistently underestimate the measured summertime concentrations by far more than a factor of 2. This indicates that at high latitudes the emissions of reactive NMHC are underestimated in the model by far more than a factor of 2. However, the absolute

strength of regional sources required to maintain the small measured summertime mixing ratios of reactive NMHC is very small compared to the total global emissions rates for these NMHC.

[48] Our results show a significant decrease in the atmospheric concentrations of several NMHC during the study period. They are higher for more reactive NMHC, and there is evidence that the trends are more pronounced in summer than in winter. The most likely explanation is a decrease in emission rates at high latitudes. However, as mentioned above, present NMHC emission inventories for high latitudes are inadequate to model our observation and we therefore have to accept that our understanding of high latitude NMHC sources is incomplete. Nevertheless, our study period overlaps with the period of major economic changes in Russia and the former Soviet Union. Changes in industrial activities as well as in oil and gas exploitation in Siberia may therefore be one of the possible reasons for changes in NMHC emission rates at high northern latitudes.

## References

- Atkinson, R., Kinetics and mechanism of the gas phase reactions of the hydroxyl radical with organic compounds under atmospheric conditions, *Chem. Rev.*, **86**, 69, 1986.
- Atkinson, R., D. L. Baulch, R. A. Cox, R. F. Hampson, J. A. Kerr, M. J. Rossi, and J. Troe, Evaluated kinetic, photochemical and heterogeneous data for atmospheric chemistry, Supplement V, IUPAC subcommittee on gas kinetic data evaluation for atmospheric chemistry, *J. Phys. Chem. Ref. Data*, **26**, 215–290, 1997a.
- Atkinson, R., D. L. Baulch, R. A. Cox, R. F. Hampson, J. A. Kerr, M. J. Rossi, and J. Troe, Evaluated kinetic, photochemical and heterogeneous data for atmospheric chemistry, Supplement V, IUPAC subcommittee on gas kinetic data evaluation for atmospheric chemistry, *J. Phys. Chem. Ref. Data*, **26**, 521–1011, 1997b.
- Blake, D. R., and F. S. Rowland, Continuing worldwide increase in tropospheric methane, 1978 to 1987, *Science*, **239**, 1129–1131, 1988.
- Boudries, H., G. Toupance, and A. L. Dutot, Seasonal variation of atmospheric nonmethane hydrocarbons on the western coast of Brittany, France, *Atmos. Environ.*, **28**, 1095–1112, 1994.
- Canadian Baseline Program, *Summary of Progress to 1998*, edited by G. McBean, Atmos. Environ. Serv., Environ., Canada, Toronto, 1999.
- Davison, A. C., and D. V. Hinkley, *Bootstrap Methods and Their Application*, Cambridge Series in Statistical and Probabilistic Mathematics, Cambridge Univ. Press, New York, 1997.
- Derwent, R. G., P. G. Simmonds, S. O'Doherty, and D. B. Ryall, The impact of the Montreal protocol on halocarbon concentrations in Northern Hemisphere baseline and European air masses at Mace Head, Ireland, over a ten year period from 1987–1996, *Atmos. Environ.*, **32**, 3689–3702, 1998.
- Dlugokencky, E. J., K. A. Masarie, P. M. Lang, P. P. Tans, L. P. Steele, and E. G. Nisbet, A dramatic decrease in the growth rate of atmospheric methane in the Northern Hemisphere during 1992, *Geophys. Res. Lett.*, **21**, 45–48, 1994.
- Dlugokencky, E. J., L. P. Steele, P. M. Lang, and K. A. Masarie, Atmospheric methane at Mauna Loa and Borrow observatories: Presentation and analysis of in situ measurements, *J. Geophys. Res.*, **100**, 23,103–23,113, 1995.
- Efron, B., *The Jackknife, the Bootstrap and Other Resampling Plans*, J. W. Arrowsmith, Bristol, England, 1982.
- Efron, B., and R. J. Tibshirani, *An Introduction to the Bootstrap*, Chapman and Hall, New York, 1983.
- Ehhalt, D. H., Gas phase chemistry of the troposphere, in *Global Aspects of Atmospheric Chemistry*, edited by R. Zellner, pp. 21–109, Springer-Verlag, New York, 1999.
- Ehhalt, D. H., U. Schmidt, R. Zander, Ph. Demoulin, and C. P. Rinsland, Seasonal cycle and secular trends of the total and tropospheric column abundance of ethane above the Jungfraujoch, *J. Geophys. Res.*, **96**, 4985–4994, 1991.
- Gautrois, M., and R. Koppmann, Diffusion technique for the production of gas standards for atmospheric measurements, *J. Chromatogr. A*, **848**, 239–249, 1999.
- Hansen, J., G. Russel, D. Rind, P. Stone, A. Lacis, S. Lebedeff, R. Ruedy, and L. Travis, Efficient three-dimensional global models for climate studies: Models I and II, *Mon. Weather Rev.*, **111**, 609–662, 1983.

- Jobson, B. T., Z. Wu, H. Niki, and L. A. Barrie, Seasonal trends of isoprene, C<sub>2</sub>-C<sub>5</sub> alkanes, and acetylene at a remote boreal site in Canada, *J. Geophys. Res.*, **99**, 1589–1599, 1994.
- Khalil, M. A. K., and R. A. Rasmussen, Atmospheric methane in the recent and ambient atmosphere: Concentrations, trends, and interhemispheric gradient, *J. Geophys. Res.*, **89**, 11,599–11,605, 1984.
- Khalil, M. A. K., and R. A. Rasmussen, Atmospheric methane: Trends over the last 10,000 years, *Atmos. Environ.*, **26**, 2445–2452, 1987.
- Khalil, M. A. K., and R. A. Rasmussen, Carbon monoxide in the Earth's atmosphere: Indications of a global increase, *Nature*, **332**, 242–245, 1988.
- Khalil, M. A. K., and R. A. Rasmussen, The global cycle of carbon monoxide: Trends and mass balance, *Chemosphere*, **20**, 227–242, 1990.
- Khalil, M. A. K., and R. A. Rasmussen, Global decrease in atmospheric carbon monoxide concentration, *Nature*, **370**, 639–641, 1994.
- Khalil, M. A. K., and R. A. Rasmussen, Atmospheric methyl chloride, *Atmos. Environ.*, **33**, 1305–1321, 1999.
- Krol, M., P. J. Van Leuwen, and J. Lelieveld, Global OH trend inferred from methylchloroform measurements, *J. Geophys. Res.*, **103**, 10,697–10,711, 1998.
- Laurila, T., and H. Hakola, Seasonal cycle of C<sub>2</sub>-C<sub>5</sub> hydrocarbons over the Baltic Sea and northern Finland, *Atmos. Environ.*, **30**, 1597–1607, 1996.
- Lindskog, A., and J. Moldanová, The influence of the origin, season and time of the day on the distribution of individual NMHC measured at Rörvik, Sweden, *Atmos. Environ.*, **28**, 2383–2398, 1994.
- McCulloch, A., M. L. Aucott, T. E. Graedel, G. Kleiman, P. M. Midgley, and Y.-F. Li, Industrial emissions of trichloroethene, tetrachloroethene, and dichloromethane: Reactive Chlorine Emissions Inventory, *J. Geophys. Res.*, **104**, 8417–8427, 1999.
- McLaren, R. D. L. Singleton, J. Y. K. Lai, B. Khouw, E. Singer, Z. Wu, and H. Niki, Analysis of motor vehicle sources and their contribution to ambient hydrocarbon distributions at urban sites in Toronto during the Southern Ontario Oxidant Study, *Atmos Environ.*, **30**, 2219–2232, 1996.
- Montzka, S. A., J. H. Butler, R. C. Myers, T. M. Thompson, T. H. Swanson, A. D. Clarke, L. T. Lock, and J. W. Elkins, Decline in the tropospheric abundance of halogen from halocarbons: Implications for stratospheric ozone depletion, *Science*, **272**, 1318–1322, 1996.
- Mylona, S., EMEP emission data status report 1999, *Res. Rep. 26*, Norw. Meteorol. Inst., Oslo, 2000.
- Novelli, P. C., L. P. Steele, and P. P. Tans, Mixing ratios of carbon monoxide in the troposphere, *J. Geophys. Res.*, **97**, 20,731–20,750, 1992.
- Novelli, P. C., K. A. Masarie, P. P. Tans, and P. M. Lang, Recent changes in atmospheric carbon monoxide, *Science*, **263**, 1587–1590, 1994.
- Novelli, P. C., K. A. Masarie, and P. M. Lang, Distributions and recent changes of carbon monoxide in the lower troposphere, *J. Geophys. Res.*, **103**, 19,015–19,033, 1998.
- Olivier, J. G. J., A. F. Bouwman, C. W. M. Van der Maas, J. J. M. Berdowski, C. Veldt, J. P. J. Bloos, A. J. H. Visschedijk, P. Y. J. Zandveld, and J. L. Haverlag, Description of EDGAR version 2.0: A set of global emission inventories of greenhouse gases and ozone-depleting substances for all anthropogenic and most natural sources on a per country basis and on 1 × 1 grid, *Rep. 771060 002/TNO-MEP Rep. R96/119*, Natl. Inst. of Public Health and the Environ. (RIVM), Bilthoven, Netherlands, 1996.
- Penkett, S. A., N. J. Blake, P. Lightman, A. R. W. Marsh, P. Anwyl, and G. Butcher, The seasonal variation of nonmethane hydrocarbons in the free troposphere over the North Atlantic Ocean: Possible evidence for extensive reaction of hydrocarbons with the nitrate radical, *J. Geophys. Res.*, **97**, 2865–2885, 1993.
- Prather, M., and D. H. Ehhalt, Atmospheric chemistry and greenhouse gases, in *Climate Change 2001: The Scientific Basis*, edited by J. T. Houghton et al., pp. 239–288, Cambridge Univ. Press, New York, 2001.
- Prather, M. J., M. B. McElroy, S. C. Wofsy, G. Russel, and D. Rind, Chemistry of the global troposphere: Fluorocarbons as tracers of air motion, *J. Geophys. Res.*, **92**, 6579–6613, 1987.
- Press, W. H., S. A. Teukolsky, W. T. Vetterling, and B. P. Flannery, *Numerical Recipes*, 2nd ed., pp. 666–671, Cambridge Univ. Press, New York, 1992.
- Prinn, R. G., et al., Evidence for substantial variations of atmospheric hydroxyl radicals in the past two decades, *Science*, **292**, 1882–1888, 2001.
- Ramacher, B., J. Rudolph, and R. Koppmann, Hydrocarbon measurements in the spring arctic troposphere during the ARCTOC 95 campaign, *Tellus, Ser. B*, **49**, 466–485, 1997.
- Ramacher, B., J. Rudolph, and R. Koppmann, Hydrocarbon measurements during tropospheric ozone depletion events: Evidence for halogen atom chemistry, *J. Geophys. Res.*, **104**, 3633–3653, 1999.
- Rudolph, J., The tropospheric distribution and budget of ethane, *J. Geophys. Res.*, **100**, 11,369–11,381, 1995.
- Rudolph, J., Biogenic sources of atmospheric alkenes and acetylene, in *Biogenic Volatile Organic Compounds in the Atmosphere*, edited by G. Helas, J. Slanina, and R. Steinbrecher, pp. 53–65, SPB Acad., Amsterdam, 1996.
- Rudolph, J., A. Khedim, T. S. Clarkson, and D. Wagenbach, Long-term measurements of light alkanes and acetylene in the Antarctic troposphere, *Tellus, Ser. B*, **44**, 252–261, 1992.
- Spivakovskiy, C. M., et al., Three-dimensional climatological distribution of tropospheric OH: Update and evaluation, *J. Geophys. Res.*, **105**, 8931–8980, 2000.
- Steele, L. P., E. J. Dlugokencky, P. M. Lang, P. P. Tans, R. C. Martin, and K. A. Masarie, Slowing down of global accumulation of atmospheric methane during the 1980's, *Nature*, **358**, 313–316, 1992.
- Trivett, N. B. A., D. E. J. Worthy, and K. A. Brice, Surface measurements of carbon dioxide and methane at Alert during an arctic haze event in April, 1986, *J. Atmos. Chem.*, **9**, 383–397, 1989.
- U.S. Environmental Protection Agency, National air pollutant emission trends 1900–1996, *EPA Rep. EPA-600/R-98-047*, Washington, D. C., 1998.
- Zander, R., Ph. Demoulin, D. H. Ehhalt, U. Schmidt, and C. P. Rinsland, Secular increase of the total vertical column abundance of carbon monoxide above central Europe since 1950, *J. Geophys. Res.*, **94**, 11,021–11,028, 1989.

T. Brauers, M. Gautrois, R. Koppmann, F. Rohrer, and O. Stein, Institut für Chemie und Dynamik der Geosphäre, Institut II: Troposphäre, Forschungszentrum Jülich, Postfach 1913, Leo Brandt Straße, Jülich D-52428, Germany. (r.koppmann@fz-juelich.de)

J. Rudolph, Chemistry Department and Centre for Atmospheric Chemistry, York University, 4700 Keele Street, Toronto, Ontario, Canada M3J 1P3.